# Contact-fatigue of High Precision Machined Surfaces

**Alexis Gautier[a], Philippe Revel[a], Henri-Paul Lieurade[b], Guillaume Thoquenne[b]**

[a] Laboratoire Roberval (FRE 2833) Université de Technologie de Compiègne, France
[b] CETIM, Senlis, France

**Abstract** Surface state, resulting from manufacturing processes, has a significant impact on product performances, such as fatigue resistance of parts. The contact-fatigue life is a function of roughness, structural phases and residual stresses level. High precision machining allows to reach surface quality which have an equivalent roughness to those obtained after successive operations such as turning and grinding. Furthermore, the material surface could be strongly in compression, which is an advantageous state. In order to measure surfaces, before and after contact-fatigue tests, accurate techniques of analysis were used such as interferometric microscopy, X-Ray diffraction and EDXD.

***Keywords**: High precision machining; Surface characterization; Interferometric microscopy; X-Ray diffraction; Contact-fatigue.*

## 1 INTRODUCTION

In optical and mechanical industries, part dimensions go typically from millimeters to centimeters. The choice of manufacturing processes depends on material properties, part geometry, performances to achieve and the unit cost. For revolved-parts the typical sequence is: turning to obtain the main form of the part, grinding to control the dimensional tolerances and to improve roughness. With High Precision Turning (HPT), these two steps can be reduced to one. However, functionality of part surface, such as fatigue lifetime, depends on their integrity. This requirement allows to use a "superfinishing" process and to characterise morphologically (form, roughness, etc.) and structurally (phases, residual stresses, etc.) machined surfaces.

In the first part of this paper, HPT technique is presented, then in the second part surface characterization techniques are described. Finally, some results of machining parts and contact-fatigue tests are presented and discussed.

## 2 EXPERIMENTAL PROCEDURE

### 2.1 Material and High Precision Machining

Rolling surfaces, which are usually in hard steel such as AISI 52100 (100Cr6), are submitted to contact-fatigue solicitation. To improve their performances, HPT process is tested.

The high precision machine (Fig. 1) is a prototype lathe* located in an air-conditioned room. The two slide ways are fixed on a massive granite block (1.5 tons) resting on four self-levelling pneumatic isulators. The slide-ways are guided by hydrostatic bearings, offering low friction, high stiffness and damping. The straightness of each one is under 0.3 µm for more than 100 mm of displacement. Linear motors (ILD-Etel™) allow to reach strong dynamic stiffness in order to reduce the number of machine elements, and to limit parasitic forces. Otherwise, displacements are measured by two optical encoders (LIP 101-Heindenhain™) of 4 nm resolution and controlled by an accurate Computer Numerical Control system (PMAC-Deltatau™). A magnetic-bearing spindle with active servo control is located on the z-axis slide-way [1,2]; the specimen is fixed in front of the spindle.

* This machine was designed by SNECMA-motors company, with the financial support of DRET (Direction de la Recherche des Etudes et Techniques).

The geometrical and dimensional aspects of parts greatly depend on the displacement and control qualities of the machine, whereas the surface integrity (roughness and residual stresses) is mainly due to the interaction between the tool and the machined material, but also due to the machine stiffness. The most performing tool is single crystal diamond tool (SCD), which gives exceptional surface integrity due to its highest hardness, high thermal conductivity and sharp edge [3]. However, due to the chemical reaction between carbon of the diamond and iron, this tool material is forbidden for steel machining. Consequently, other tool materials such as aluminium ceramics or cubic Boron Nitride (cBN) are required. Otherwise, in case of high carbon steels, dry machining is required in order to create a hot point that softens material.

Machining parameters (Tab. I) were optimized to obtain the best roughness results according to our experience and bibliographical results [4,5,6].

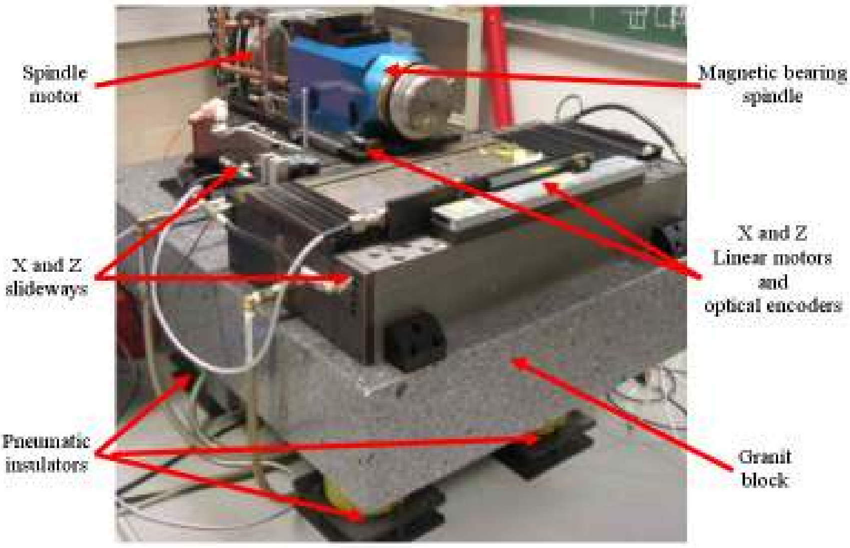


Figure 1: UTC High Precision Turning machine.

## 2.2 Contact-fatigue Process

Contact-fatigue tests are carried out on a special machine (Fig. 2). Rolling samples are mounted on two axis and submitted to contact-fatigue under lubrication with or without sliding during a programmed cycle number. The desired contact pressure is given by a pneumatic actuator. There are two steps during contact-fatigue test: the first is the running-in which is the accommodation of samples surfaces and the stabilization of the surface integrity. The second step is the contact-fatigue test until the rolling sample pitting (detected by an Hall effect sensor).

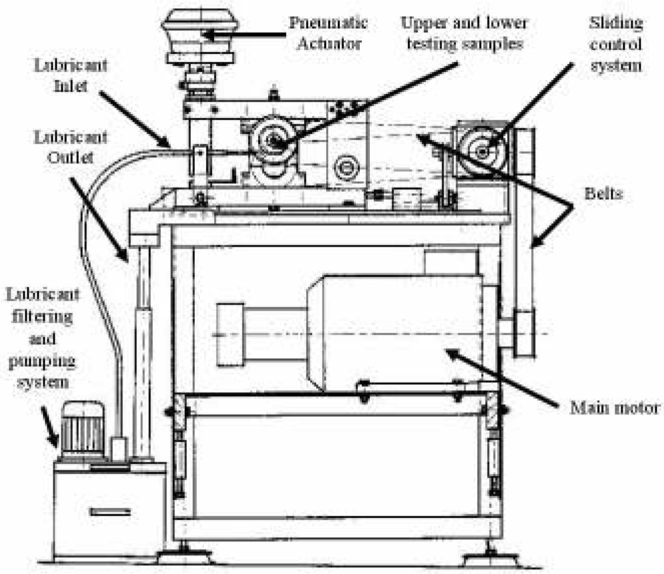


Figure 2: CETIM contact-fatigue test machine.

## 2.3 Surface Characterization

Roughness surface measurements were performed with an optical technique which displays in a short time (less than one minute) a local three-dimensional topography of a surface without any contact. In this study, an interferometric microscope (New View 200-ZYGO™) with white light wavelength is used to measure machined surfaces. The vertical resolution (z) is about 0.1 nm and the lateral resolution (x-y) is respectively 1.1 µm for the objective (x 10) and 4.4 µm for (x 2.5). The measured surface areas according to the objective are between 0.37 and 5.95 mm2. Arithmetic roughness (Ra) and maximum peak to valley value (Rt) are computed from the measures.

Measurement of residual stresses was carried out by classical X-ray diffraction with a 4-axis goniometer, for each direction (feed and cutting directions) tensile and shear stresses are measured. The Full Width at Half Maximum (FWHM) is given to assess the material work hardening level.

Phases measurement, such as retained austenite, was not performed by classical X-Ray diffraction (measurement of (200) austenite and marsensite doublet (211)(112) peaks), but by an original method: the EDXD (Energy Dispersion by X-Ray Diffraction). This analysis uses the full spectrum of the observed material. Phases content is determined by the energy discrepancy in function of wavelength. In our study, phases analysed are austenite, martensite and carbides ($Fe_3C$).

The experimental study was conducted in two steps. Firstly, three specimens (S1, S2, S3) were machined and analysed in order to compare their surface integrity with grinded surfaces. Secondly, four other samples (S4, S5, S6, S7) were machined and tested in contact-fatigue until the end of running-in step; they were structurally characterized before and after running-in step.

# 3 RESULTS AND DISCUSSION

Samples S1 and S3 were used to assess the tool material: S1 was machined with a monolithic carbide cutting tool, whereas S3 was machined with same cutting parameters but using a cBN cutting tool. Roughness, phases content and surface residual stresses after machining are presented in table I. S2 and S3 were machined with different feed rates.

Table I: Characterization results of HPT samples S1, S2 and S3 with these cutting parameters: $V_c$ = 300 m/min. (cutting speed), $a_p$ = 30 µm (cutting depth), $r_\varepsilon$ = 0.4 mm (tool radius nose).

| Sample | Bulk material | S1 | S2 | S3 |
|---|---|---|---|---|
| Cutting tool material | - | Carbide | cBN | cBN |
| Feed rate (µm/rev.) | - | 4.4 | 13.2 | 4.4 |
| Ra (µm) | - | 0.8 | 1.2 | 0.6 |
| Martensite phase (%) | 95.33 (+/- 0.74) | 72.76 (+/- 0.61) | 81.43 (+/- 0.62) | 87.82 (+/- 0.63) |
| Carbide phase (%) | 4.59 (+/- 0.89) | 9.41 (+/- 0.89) | 12.71 (+/- 0.86) | 7.84 (+/- 0.81) |
| Austenite phase (%) | 0.08 (+/- 0.27) | 17.82 (+/- 0.47) | 5.86 (+/- 0.39) | 4.35 (+/- 0.37) |
| Surface residual stress in feed direction (MPa) | - | -1253 | -1445 | -1329 |
| Surface residual stress in cutting direction (MPa) | - | -303 | -215 | -92 |
| Full Width at Half Maximum | - | 7.57 | 6.86 | 6.24 |

According to these results, different observations could be done:

- All machined surfaces show an increase of carbide and austenite content compared to the bulk material. During machining, cutting pressures and high temperatures (due to dry cutting) generate metallurgical transformations. By comparison of S1 and S3 phases content, a great influence of cutting tool material is observed on metallurgical transformations, especially the austenite transformation. Only the cBN cutting tool is available to have a retained austenite content lower than 6 % (upper limit of austenite content accepted by bearing manufacturers). This effect is mainly due to the difference of thermal properties of the cutting tool material: cBN has a coefficient of thermal conductivity higher than carbide one [4,5,7,8].

- S1 and S3 roughnesses are quite similar. But cBN cutting tool is well known to have a better cutting lifetime [4,9,10] than carbide tools in case of hard steel machining.
- The comparison of S2 and S3 samples indicates that roughness increases with feed rate, whereas phases content and residual stresses are not affected.
- The compression residual stresses in feed direction are larger than those in cutting direction.
- The work hardening (FWHM value) is higher on surface machined by a carbide cutting tool than those machined by a cBN cutting tool. This work hardening result is related to hardness of the cBN cutting tool which allow a better material cutting.

Surface characterization is not sufficient to determine or predict the behaviour in contact-fatigue; a structural characterization below to the surface is also necessary. In-depth residual stresses profiles were measured by using X-ray Diffraction after controlled electro-chemical etchings. Residual stresses in the feed direction are presented (Fig. 3).

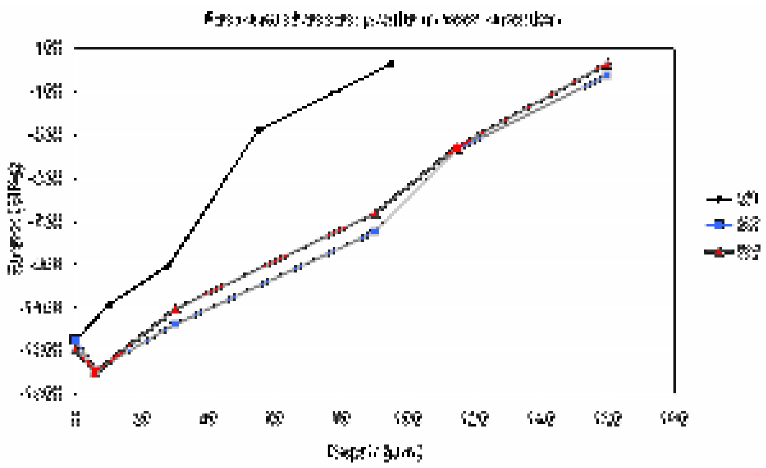

Figure 3: In-depth residual stresses profiles in feed direction of HPT machined samples (S1 with a carbide cutting tool and S2/S3 with a cBN cutting tool) according to cutting parameters of table 1.

According to these results, different observations could be done:

- The profiles of S2 and S3 (cBN cutting tool) are very similar. Therefore, feed rate effect is not significant for the selected values.
- The cBN tool leads to larger compressive depth as compared with the carbide tool.
- The compression zone is also deeper in case of cBN cutting tool (160 µm for cBN, versus 100 µm for carbide tool). Therefore, considering the residual stresses level and phases content, use of cBN cutting tool seems to be better than carbide cutting tool.

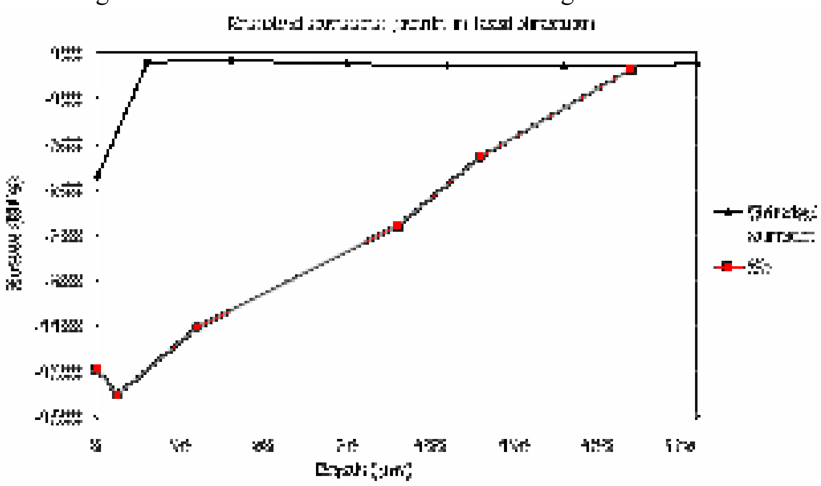

Figure 4: In-depth residual stresses profiles of HPT machined (S3) sample and a grinded sample.

Curves of figure 4 show the main difference about residual stresses profiles of the two processes (HPT and grinding): residual stresses of HPT machined surface are more in compression and also deeper below to the surface. This kind of profile is greatly advantageous for contact-fatigue lifetime.

To balance these results, grinded surface roughness (Ra = 0.2 µm) is lower than HPT surface roughness (Ra = 0.6 µm). Then, optimization of HPT process could be done in order to perform the roughness without damaging the material structural state.

After an optimization of cutting parameters in regard of roughness, other samples (S4, S5, S6, S7) were machined in order to be tested in running-in contact-fatigue (cutting parameters of S4 and S5 were the same, and S6 and S7 too). The contact-fatigue parameters of the running-in were 100,000 cycles, 3.5 GPa equivalent pressure without sliding. Surface residual stresses measures and phases analyses were realized before and after the running-in (Tab. II).

Table II: Surface characterization results of HPT samples S4, S5, S6 and S7 with these cutting parameters: $V_c$ = 500 m/min. (cutting speed), $a_p$ = 6 µm (cutting depth), $r_\varepsilon$ = 0.8 mm (tool radius nose).

| Sample | S4 | S5 | S6 | S7 |
|---|---|---|---|---|
| Feed rate (µm/rev.) | 49 | 49 | 160 | 160 |
| Ra (µm) | 0.45 | 0.47 | 0.42 | 0.54 |
| Martensite phase before F.C. (%) | 89.6 | 89.8 | 84.1 | 84.2 |
| Martensite phase after F.C. (%) | 89.9 | 91.0 | 84.1 | 84.5 |
| Carbide phase before F.C. (%) | 8.5 | 8.6 | 10.7 | 10.4 |
| Carbide phase after F.C. (%) | 8.8 | 7.9 | 11.3 | 11.0 |
| Austenite phase before F.C. (%) | 1.9 (+/- 0.2) | 1.6 (+/- 0.2) | 5.2 (+/- 0.3) | 5.4 (+/- 0.3) |
| Austenite phase after F.C (%) | 1.3 (+/- 0.3) | 1.1 (+/- 0.3) | 4.6 (+/- 0.3) | 4.5 (+/- 0.3) |
| Residual stress in feed direction before F.C. (MPa) | -231 (+/- 20) | -476 (+/- 17) | -760 (+/- 17) | -809 (+/- 18) |
| Residual stress in feed direction after F.C. (MPa) | -545 (+/- 16) | -751 (+/- 16) | -701 (+/- 14) | -811 (+/- 18) |
| Residual stress in cutting direction before F.C. (MPa) | 39 (+/- 17) | -27 (+/- 16) | -42 (+/- 16) | -179 (+/- 16) |
| Residual stress in cutting direction after F.C. (MPa) | -349 (+/- 14) | -384 (+/- 15) | -66 (+/- 13) | -148 (+/- 17) |
| Full Width at Half Maximum before F.C | 6.46 (+/- 0.16) | 6.34 (+/- 0.15) | 7.09 (+/- 0.15) | 6.71 (+/- 0.13) |
| Full Width at Half Maximum after F.C. | 6.15 (+/-0.16) | 6.40 (+/- 17) | 6.71 (+/- 0.13) | 6.88 (+/- 0.14) |

According to these results, some remarks could be done:

- Results of S4 and S5 samples show a good process repeatability as well as about roughness than phases content. Phases analyses allow to observe that retained austenite is greatly lower than 6% and then, roughness optimization does not deteriorate the structural state of the material, due to the cBN tool performance. Unfortunately, a consequence of the roughness optimization is a decrease of the compressive residual stresses. After running-in contact-fatigue tests, residual stresses in feed and cutting directions are more in compression than before tests (~ -300 MPa) for S4 and S5.
- Results of S6 and S7 samples are quite similar about roughness and phases content. On the other hand, residual stresses in cutting direction are different (-42 MPa versus -179 MPa). There is no significant residual stresses evolution between before and after running-in.

- Comparison of S4/5 and S6/7 phases contents results confirms the fact that retained austenite decrease during contact-fatigue test [11]. Indeed, this phase is transformed in martensite by mechanical pressures.
- Results allow to confirm that the higher the feed rate is, the more in compression residual stresses in feed direction are.
- Despite of very different feed rates between S4/S5, versus S6/S7, the roughness results are quite the same. Moreover, by comparison between S3 and S4-7, the roughness optimization does not seem to be very significant.

Best result of roughness optimization (Fig. 5) was Ra = 0.110 µm with 30 µm cutting depth, 49 µm/rev. feed rate and 500 m/min. cutting speed. Consequently, new samples were machined with the same cutting parameters. But low frequencies were observed due to trouble on spindle close loop servo during the machining. Therefore cutting depth was decreased from 30 µm to 6 µm in order to attenuate this trouble (samples S4-7, Fig.6).

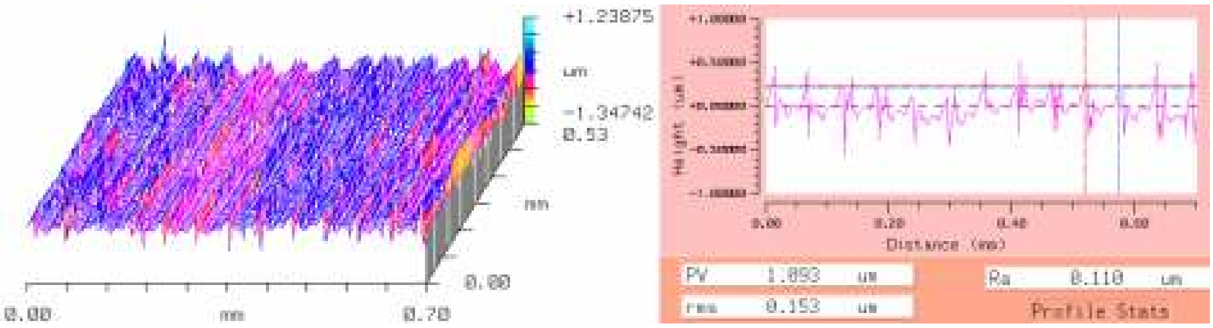


Figure 5: 3D topographic picture and profile of S8 sample (Ra = 0.110 µm).

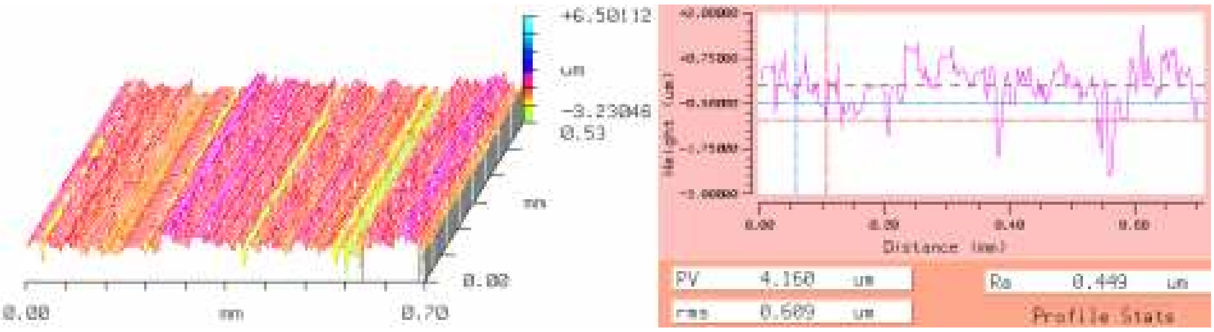


Figure 6: 3D topographic picture and profile of S4 sample (Ra = 0.449 µm).

Figure 5 profile is very periodic: the measured period (between inspector lines) is about 52 µm which is closer than the feed rate (49 µm/rev.). Despite of the cutting depth decrease (30 µm to 6 µm), roughness profiles (S4-7) are still disturbed. This is evidenced on figure 6 profile by the unviewable pitch (pitch is usually consequence of feed rate). This effect is due to the spindle close loop servo trouble. In order to comfort this statement, a "high pass" filter was applied (in order to remove the waviness default) on S4 topographic data (Fig. 7). The Ra of S4 filtered (0.132 µm) is then quite equal to the one of S8 (0.110 µm, Fig. 5); these results confirm the remark about spindle close loop trouble and its consequence on roughness results of the table II.

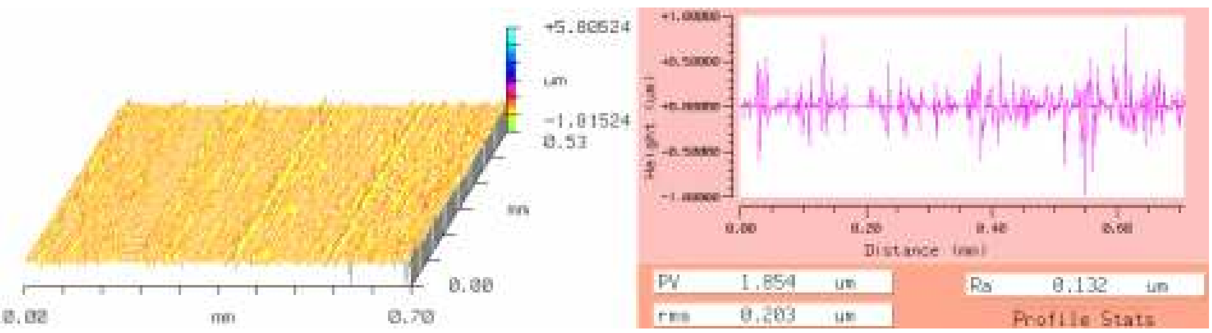


Figure 7: 3D topographic picture and profile of S4 sample with "high pass" filtering (Ra = 0.132 µm).

# 4 CONCLUSION

These first experimentations about HPT machining on AISI 52100 lead to establish these remarks:

- Results confirm that cBN is the best cutting tool material in order to machine hard bearing steel because of better structural state (lower percentage of retained austenite, deeper compression zone) and better machining life [7] than carbide cutting tool.
- Selected cutting parameters modify the surface integrity (roughness, residual stresses and phases content) and then improve the process in regard of contact-fatigue running-in.
- Surface integrity of HPT samples could be more efficient with the contact-fatigue tests than classical grinded surfaces (due to the higher and deeper compressive zone).
- Roughness of HPT surfaces can be lower (0.110 µm) than classical grinded surface (0.200 µm), according to a good process repeatability.
- In function of the initial residual stresses level, different kind of residual stresses evolutions could be observed during running-in contact-fatigue test.

These results give some directions for future studies:

- Perform the spindle close loop servo.
- Pursuit contact-fatigue tests until pitting of samples in order to compare life of HPT surfaces to those obtained by grinding.
- Compare residual stresses profiles at each life step (after machining, after running-in, after pitting) of a rolling surface in order to observe and understand the evolution of material from machining to end of contact-fatigue test.
- Optimize cutting parameters in order to find the best contact-fatigue life.
- Determinate a roughness parameter which could be more pertinent to characterize contact-fatigue lifetime than classical roughness parameters such as Ra, Rq.

# 5 ACKNOWLEDGEMENTS

The authors thank the Picardie Region Council for its financial support.

# 6 REFERENCES:

1. C. Fouché, J.-P. Marioge, M. Mullot, Magnetic bearing spindle application on high precision turning. (In French: Application de la broche à paliers magnétique à l'usinage de très haute précision), Revue Scientifique et Technique de la Défense, 1988, 99-109.
2. H. Khanfir, M. Bonis, P. Revel, Improving waviness in ultra precision turning by optimizing the dynamic behaviour of a spindle with magnetic bearings. International Journal of Machining Tools Manufacturing, 2005, 45, 841-848.
3. P. Revel, H. Khanfir, R.Y. Fillit, Surface characterization of aluminium alloys after diamond turning. J. Material Processing Techniques, 2006, 178, 154-161.
4. G. Poulachon, Aspect phénomenologiques, mécaniques et métallurgiques en tournage c-BN des aciers durs, PhD thesis, ENSAM Cluny, 1999.
5. M. Jacobson, Hard turning of bearing steels controlling residual stress and improving fatigue life, PhD thesis, Chalmers University of Technology, 2004.
6. M. A. Yallese, L. Boulanouar, Kamel Chaoui, Usinage de l'acier 100Cr6 trempé par un outil en nitrure de bore cubique, Mécanique et Industries, 2004, 5, 355-368.
7. G. Poulachon, B. P. Bandyopadhyay, I. S. Jawahir, S. Pheulpin, E. Seguin, Wear beahavior of CBN tools while turning various hardened steels, Wear, 2004, Elsevier, 256, 301-310.
8. G. Poulachon, A. Albert, M. Schluraff, I. S. Jawahir, An experimental investigation of work microstructure effects on white layer formation in PCBN hard turning, Machine Tools and Manufacture, 2005, Elsevier, 45, 211-218.
9. J. Hua, R. Shivpuri, X. Cheng, V. Bedekar, Y. Matsumoto, F. Hashimoto, T. R. Watkins, Effect of feed rate, workpiece hardness and cutting edge on subsurface residual stress in hard turning of bearing steel using chamfer + hone cutting edge geometry, Material Science and Engineering, 2005, Elsevier, A 394, 238-248.

10. Y. K. Chou, C. J. Evans, M. M. Barash, Experimental investigation on CBN turning of hardened AISI 52100 steel, Materials Processing Technology, 2003, Elsevier, 134, 1-9.
11. R. C. Dommarco, K. J. Kozaczek, P. C. Bastias, G. T. Hahn, C. A. Rubin, Residual stresses and retained austenite distribution and evolution in SAE 52100 steel under rolling contact loading, NDE Engineering Codes and Standards and Materials Characterization, 1996, ASME, PVD 322 NDE 15.